THE STRENGTH OF JIS SNCM8 STEEL UNDER COMBINED ALTERNATING STRESSES

K. Tanaka and S. Matsuoka*

INTRODUCTION

The most extensive fatigue tests under combined loading were conducted before 1955. These were mainly due to Gough [1], Nishihara [2] and Findley [3]. The testing machines used by all of them were mechanically driven and the tests were performed under the combination of bending and torsion. Since fatigue failure results from plastic deformation of all or a part of material, it is reasonably anticipated that some of generally accepted yield criteria for ductile materials should also correlate fatigue results under combined stress states. However, it has not been conclusively shown that fatigue under combined stress follows any of the common theories of failure. One of the reasons for this may reside in the fact that most of the analyses were based on the data obtained by the combination of bending and torsion [1-3]. In this case, the specimen is subjected to a stress gradient and an ideal biaxial stress state is not available. Another difficulty in the formulation of the criterion follows from the fact that the tests involve a large number of specimens and that a considerable amount of statistical scatter is inevitable in the resulting data due to the inherent nature of fatigue failure.

This work presents the results of tests on JIS SNCM8 steel under combined axial loading and torsion by using hollow and solid cylindrical specimens. The tests on hollow specimens would give the intrinsic fatigue strength under biaxial stress states. The tests on solid specimens would reveal the effect of a stress gradient through the specimen. The material was selected because the statistical properties of the fatigue data for the same material had already been examined in our laboratory (NRIM)[4].

EXPERIMENTS

The machine used in these tests was an MTS electrohydraulic axial torsional testing machine with an axial force of 0.3MN and a torsional capacity of ±5kN-m. The two loading systems are controlled by two independent servo-loops and the feedback for them is from a single transducer, which ensured a cross-talk less than 1 per cent. The coupling system between the rotary actuator and the linear actuator consists of a combination of roller and thrust bearings, and which is flexible in the axial direction and stiff radially. Tests were carried out under load control with complete reversal so as to hold the stress ratio, τ_a/σ_a, constant at the surface of a specimen, where τ_a and σ_a are shear and axial stress amplidudes, respectively. The stress values employed were nominal stresses determined from an ordinary elastic solution. The research program involved 5 test series for each of hollow and solid specimens, i.e. τ_a/σ_a values; 0(axial loading), 1/4, $1/\sqrt{3}$, $\sqrt{3}$, ∞(torsion). The machine was run at 0.5 - 5 Hz and stopped when specimens

*National Research Institute for Metals, Tokyo, Japan.

failed completely or when they survived $2x10^6$ cycles.

The JIS SNCM8 steels tested were from two different heat lots by the same manufacturer and supplied in the forms of 75 mm and 35 mm diameters hot-rolled bars. The ladle analysis of the steels shown in Table 1. The steels were heat treated for 30 minutes at 845°C, then oil quenched, followed by tempering for 2 hours at 600°C and water quenching. The dimension of specimens at the gage part is shown in Table 2, where D and d are the external and internal diameters, respectively, and L is the length. Series A and B specimens were made from lot I steel and used for the main tests under combined loading and their geometries are illustrated in Figures 2 and 3, respectively. The machining of these specimens was conducted after heat-treatment of the as-received bars. Series C, D and E specimens were made from heat-lot II steel and served for preliminary tests. In the latter tests, the effect of specimen geometry was examined by changing the values of D and d, and the ratio of L/D. On the basis of the test results the geometries of the series A and B specimens were decided. The heat-treatment for the preliminary test specimens was conducted after rough-machining. The average values of Vickers hardness and the scatter (± one standard deviation) for all series of specimens are shown in the last column of Table 2. These were the values measured at the grip part of all specimens. In the case of series A and B specimens, the hardness at the gage part was lower than that at the grip part as a result of the gradient of cooling rate through specimen at the heat-treatment. Thus the estimated values relevant to the gage part were indicated in the same column. These were the values obtained in a cross section of a heat-treated 75 mm diameter bar at a position D/2 distant from the center.

The static and cyclic stress-strain relations under axial loading were determined by using series F and G specimens, being machined from 35 mm diameter bars of heat-lot I steel and heat-treated before machining and after rough-machining, respectively. The tests on these specimens were conducted in an MTS electro-hydraulic machine with a capacity of 0.15MN. The cyclic stress-strain curves were constructed by two methods; one by connecting the tips of stable hysteresis loops from companion specimens tested at different completely reversed strain ranges and the other by incremental step tests [5].

RESULTS

The monotonic and cyclic stress-strain curves under axial loading are shown in Figure 1. The material cyclic-softened drastically. Both monotonic and cyclic stress-strain behaviors for series F and G specimens were coincident with each other within the error of measurement. The static ultimate tensile strength of the material for series F specimens was 1120 MPa.

The S-N diagrams for axial loading, three combinations of axial loading and torsion, and torsion are shown in Figure 2 for hollow specimens and in Figure 3 for solid specimens. These included the results both of the main and the preliminary tests. The ordinates in the figures represent the equivalent stress amplitude, $\sigma_{eq.a}$, calculated according to the Mises criterion, i.e., $\sigma_{eq.a} = (\sigma_a^2 + 3\tau_a^2)^{1/2}$. The endurance limits for the respective series of tests corresponded to the mean strength at $2x10^6$ cycles as determined by the method standardized in JIS Z2273 (General Rules for Fatigue Testing of Metals). The S-N curves above the endurance limits for axial loading were provided commonly in the two figures by the method

of least-squares on the results of 4 hollow and 3 solid specimens in the higher stress amplitude regions. The S-N curves for torsion of hollow and solid specimens were both determined by visual inspection.

COMPARISON WITH OTHER WORK

In comparison with earlier work, the results for endurance limits in this study are plotted in Figure 4 in terms of σ_e/σ_{e0} and τ_e/σ_{e0} where σ_e and τ_e are respectively the applied amplitude of axial stresses due to axial loading and the applied amplitude of shear stresses due to torsion at the endurance limit of the combination and σ_{e0} is the endurance limit for pure axial loading. The value of σ_{e0} is the mean of the values for hollow and solid specimens and described in the insertion of Figure 4. The results of earlier work [1-3] were obtained under combined bending and torsion for quench-tempered low alloy steels, and the corresponding values of σ_e and σ_{e0} are those for bending. Results reported by Nishihara [2] and Findley [3] are for solid specimens of steels very similar to the steel tested in the present study and Gough's data [1] are for solid and hollow specimens of 3.5 per cent Ni-Cr steel.

DISCUSSION

Nishijima in NRIM examined statistically the scatter of the fatigue data of 630°C tempered SNCM8 steel under rotation bending by using more than 150 specimens [4]. He obtained the standard stress deviation of the data, s, from the mean S-N curve on a log-log plot as $s = 1.52x10^{-2}$. This value may be regarded as an estimated value of the standard stress deviation inherent to the scatter of the data in the material. The two dotted curves in Figures 2 and 3 indicate the two limits of dispersion as represented by two standard deviations of estimate according to the Nishijima's analysis; the upper one vertically on the upper side of the mean for torsion and the lower one vertically on the lower side of the mean for axial loading. The band constructed by the two dotted curves in the figures should bound more than 95 per cent of the data. At a prescribed value of τ_a/σ_a, the results for the preliminary tests provided longer lives than those from specimens for the main tests. Particularly, among the extraordinary data existing significantly outside the limits of dispersion in Figures 2 and 3, most of data were obtained from specimens for the preliminary tests. This difference probably occurred because the two series of specimens came from different heats and suffered different heat-treatments, resulting in different Vickers hardnesses at the surface of the gage part (Table 2). Therefore, if all specimens had come from the same heat and had been heat-treated in an identical manner, the data would have been less dispersed. Hence, as a conclusion, the results of the present test on the hollow and solid specimens under combined loading can be bounded by the mean S-N curve for torsion and axial loading and the associating limits of dispersion as shown in Figures 2 and 3, respectively.

In the case of hollow specimens as shown in Figure 2, the results above the endurance limits for pure torsion gave a slightly higher strength than those for pure axial loading in the high stress amplitude region. However, the S-N curve for pure axial loading represented almost coincidentally the results of combined loading. Contrary to this, the results above the endurance limits for solid specimens showed a clear stress ratio dependency as exhibited in Figure 3. They deviated more from the S-N curve for axial loading as the τ_a/σ_a-value increased and the tendency appeared stronger as

the applied stress amplitude increased. This is obviously attributed to the presence of a torsional stress gradient in the specimens resulting in a constraining of plastic deformation at the surface part due to the less strained zone of the core part. The stress gradient is highest when the solid specimens are subjected to pure torsion and the constraining effect on plastic deformation becomes higher as the shear stress amplitude increases. The occurrence of plastic deformation in the higher stress amplitude region under axial loading is evident from the cyclic stress-strain curves shown in Figure 1. Hence, if the influence of the stress gradient in torsional deformation was eliminated completely, the resulting S-N curve above the endurance limits under combined loading would yield to an S-N curve identical to one for axial loading. The condition of no-stress gradient was almost fulfilled for the case of tests on hollow specimens as shown in Figure 2.

The stress gradient and its constraining effect on plastic deformation in the surface of a specimen are higher in bending than in torsion, and thus the slope of S-N curve above the endurance limit for bending is expected to appear steeper than that for torsion. This is surely seen in Figure 3. The dash-dotted curve in the figure exhibits the mean S-N curve for bending tested by Findley [3]. When the data for combined bending and torsion due to Findley were represented by the equivalent stress amplitude on the basis of the Mises criterion, the resulting data above the endurance limits showed a good fitting with the mean S-N curve for bending. This is in contrast with the results in the present study as shown in Figure 3. The different behaviors undoubtedly follow from the different stress situations for the two types of combination.

It is evident from Figures 2 and 3 that the endurance limits under combined axial loading and torsion did not depend systematically on the shape of specimen or the associated stress gradient. This seems also to be true in the case of combined bending and torsion. It is seen in Figure 4 that the correlation between the values of σ_e/σ_{e0} and τ_e/σ_{e0} obtained in the present study is in surprisingly good agreement with that for the results tested by Findley [3]. The data of solid and hollow specimens reported by Gough [1] were slightly dependent on the shape of specimen. However, the average of the two compares well with the correlation of this study. Thus, the general tendency appearing in the endurance limits of this study can be regarded as that inherent to the ideal biaxial stress state for quench-tempered low alloy steels, being independent of the method of testing, the specimen shape or size. The results in Figure 4 indicate that, among the three failure conditions represented in the figure, the von Mises criterion gives the best agreement for the steels. Particularly when the stress ratio, τ_a/σ_a, is less than $1/\sqrt{3}$, the small deviation from the criterion can not be distinguished from that due to the scatter of the fatigue data induced from the inherent nature of the material. When τ_a/σ_a is larger than $\sqrt{3}$, the endurance limits appear clearly greater than that due to the criterion. The different strengths between the region where $\tau_a/\sigma_a \geq \sqrt{3}$ and the region where $\tau_a/\sigma_a \leq 1/\sqrt{3}$ will be certainly related to the different modes of crack propagation in the two regions. The crack in the region of the higher τ_a/σ_a-value propagated along the plane of the maximum shear stress (stage 1 crack or mode II crack), while the crack in the region of the lower one was initiated from a pore present on the surface of specimen and propagated on a plane perpendicular to the maximum tensile stress (stage 2 crack or mode I crack). As the applied stress amplitude decreases, the stage 1 crack growth in such a hard steel as tested in this study will become relatively more difficult than the stage 2 crack growth, since the stage 1 crack growth is essentially operated by slipping.

CONCLUSIONS

Fatigue tests under combined axial loading and torsion were conducted on hollow and solid specimens of quench-tempered SNCM8 steel. The results obtained were analyzed and compared with the earlier data on tests under combined bending and torsion. The fatigue strengths under combined stresses were correlated best by the von Mises criterion. The results above endurance limits depended on the shape of specimen and the method of testing. Solid specimens gave a higher strength than hollow ones as the value of τ_a/σ_a increased. The combination of axial loading and torsion gave lower slopes of the S-N curve than that of bending and torsion represented in the earlier works. The data of hollow specimens in this study were regarded as a representative indication of behavior under an ideal combined stress state, and they agreed reasonably well according to the von Mises criterion within the scatter of errors inherent to the fatigue data of the steel. However, the endurance limits appeared to be independent of the variables of testing and specimen. They tended to provide slightly greater fatigue strength in the region of high τ_a/σ_a-values than those due to the axial loading. It was suggested that the difference in the endurance limits was attributed to the difference in the modes of crack propagation.

REFERENCES

1. GOUGH, H.J. and POLLARD, H.V., Proc. I. Mech. Eng., 132, 1936, 549.
2. NISHIHARA, T. and KAWAMOTO, M., Trans. Soc. Mech. Eng., Japan, 7, 1941, 85.
3. FINDLEY, W.N., COLEMAN, J.J. and HANLEY, B.C., Proc. International Conference on Fatigue of Metals, Inst. of Mech. Eng., London, 1956, 150.
4. NISHIJIMA, S., to be published (research work in NRIM).
5. LANDGRAF, R.W., MORROW, J. and ENDO, T., J. Materials, 4, 1969, 176.

Table 1

Element / Lot No.	C	Si	Mn	P	S	Cu	Ni	Cr	Mo
I	0.40	0.25	0.63	0.029	0.020	0.13	1.68	0.68	0.18
II	0.41	0.25	0.68	0.015	0.014	0.09	1.74	0.72	0.20

Table 2

Specimen Series	External Dia. D(mm)	Internal Dia. d(mm)	Gage Length / Ext. Dia. L/D	Heat Lot (Bar Dia. in mm)	Heat Treatment *	Hardness (Hv) at the grip (at the gage part)
A	40	36	1.5	I (75)	B. M.	348.3 ± 2.7(333.3)
B	19	0	1.47	I (75)	B. M.	347.6 ± 5.7(323.3)
C	50	46	1, 2, 3	II(75)	A. M.	339.6 ± 4.3
D	35	29	1, 2	II(75)	A. M.	338.9 ± 6.1
E	20	0	1, 2	II(75)	A. M.	337.5 ± 8.6
F	10	0	1	I (35)	B. M.	344.4 ± 4.7(338.7)
G	8	0	1.25	I (35)	A. M.	341.1 ± 4.1

* B. M. : Heat-treated on as-received bars before machining
A. M. : Heat-treated after rough-machining

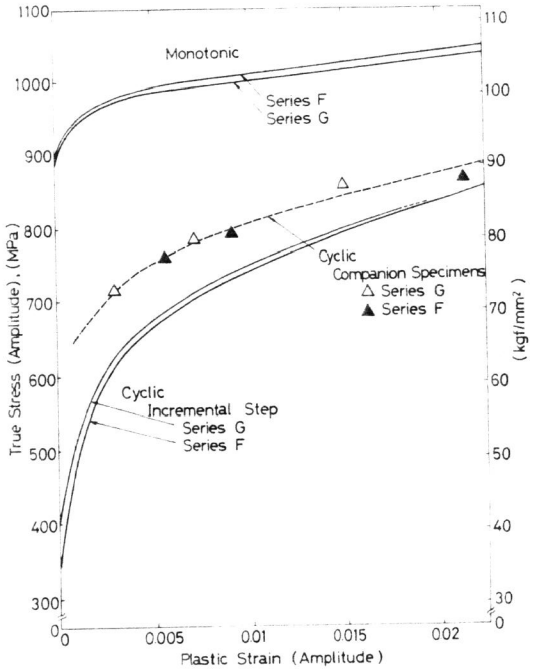

Figure 1 Monotonic and cyclic stress strain curves under axial loading for quench-tempered SNCM8 steel

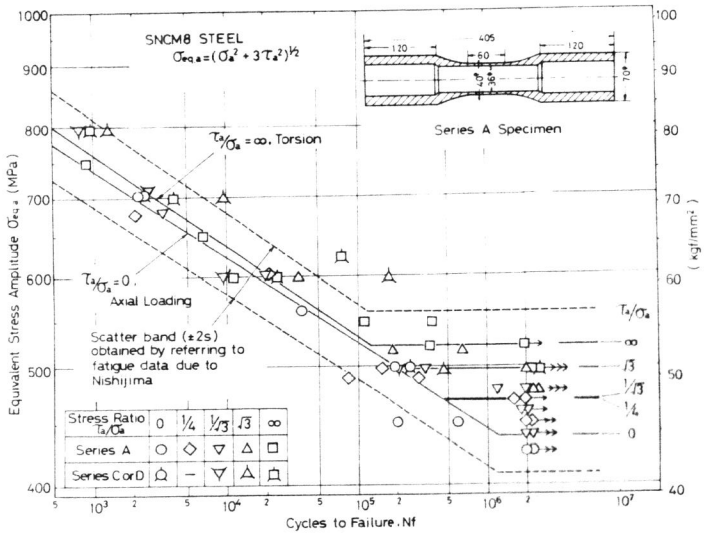

Figure 2 S-N curves under combined axial loading and torsion for hollow specimens

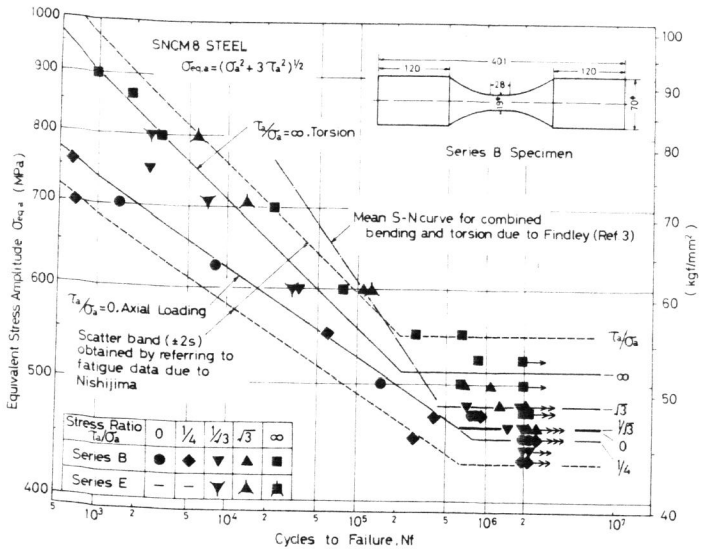

Figure 3 S-N curves under combined axial loading and torsion for solid specimens

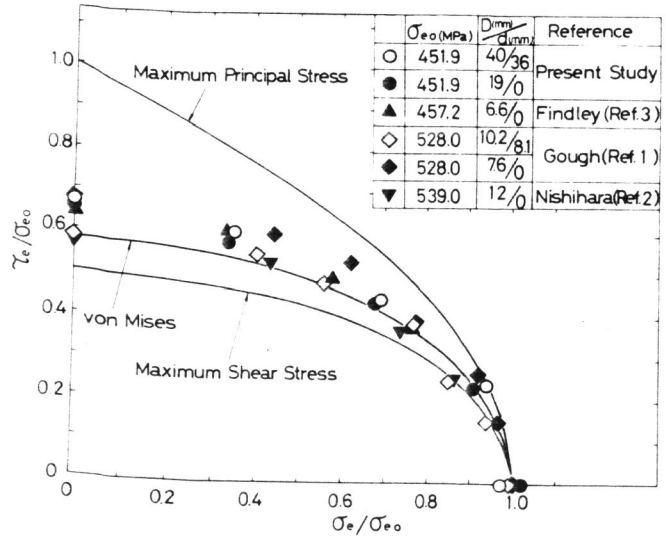

Figure 4 Criteria of failure relevent to endurance limits under combined loading